Two-Stage Multiple Access for Many Devices of Unique Identifications Over Frequency-Selective Fading Channels

Jinho Choi, *Senior Member, IEEE*

***Abstract*—In this paper, we consider sparse index multiple access for uplink random access in a wireless system of a number of devices when a fraction of them are active. This multiple access scheme is suitable for the case that an access point (AP) needs not only to receive data symbols, but also to identify active devices when there are a number of devices with unique identification sequences (the number of devices can be easily more than a million) with low signaling/control overhead. We propose a two-stage transmission scheme for random access and derive computationally efficient methods to estimate the channel state information (CSI) of active devices over frequency-selective fading channels in the first stage and to perform joint active device identification and data detection in the second stage using a well-known sparse signal estimation method in compressive sensing. Simulation results demonstrate that the proposed approach can successfully estimate the CSI of active devices under reasonable conditions and identify the unique identification sequences or vectors of active devices with a high probability. For example, when 6 out of 64 devices become active, the AP can identify all six devices (using estimated CSI) with a probability higher than $1 - 10^{-2}$ over frequency-selective fading channels.**

***Index Terms*—Compressive sensing (CS), index modulation, Internet of Things (IoT), sparsity.**

I. Introduction

THE INTERNET of Things (IoT) has attracted a great deal of attention and has been studied for standardization [1], where IoT is layered into application, service support and application support, network, and device layers. In each layer, there are a number of challenges. Among them, an important challenge is multiple access for a number of devices. For example, at homes or offices, there might be a number of devices to be connected to a gateway or access point (AP) as in Fig. 1. Thus, multiple access for a number of devices is an important issue for wireless IoT or machine type communications (MTCs) to allow multiple devices to share a physical channel of a limited bandwidth.

Manuscript received September 29, 2016; revised November 17, 2016; accepted December 2, 2016. Date of publication December 6, 2016; date of current version February 8, 2017. This work was supported by the Korea Electric Power Corporation through the Korea Electrical Engineering and Science Research Institute under Grant R15XA03-60. The material in this paper was presented in part at the 2015 IEEE Global Conference on Signal and Information Processing, Orlando, FL, USA, 2015, pp. 324–327.

The author is with the School of Electrical Engineering and Computer Science, Gwangju Institute of Science and Technology, Gwangju 61005, South Korea.

Digital Object Identifier 10.1109/JIOT.2016.2636162

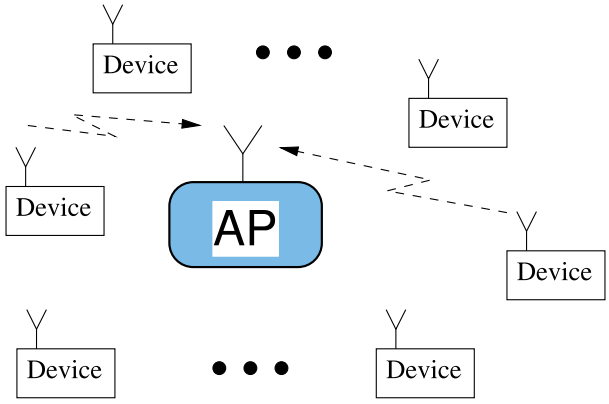

Fig. 1. System model with an AP (or gateway) and multiple devices where a subset of devices are active to transmit their data.

In [2], carrier sensing multiple access has been considered, which is widely adopted for wireless networks (e.g., WiFi). In [3] and [4], code division multiple access (CDMA) and time reversal multiple access are considered, respectively. These two multiple access schemes are also considered for multiple access in ultra-wideband (UWB) communication systems. Since UWB communications are to provide short-range wireless connections for devices, various approaches for UWB might be useful for wireless IoT as demonstrated in [4].

In wireless IoT, we may consider two different types of applications in terms of data rates [4]. The first type includes high-data-rate applications such as video streaming. In general, in this type of applications, the number of devices connected to an AP may not be large. In the second type, there are low-data-rate applications (e.g., for remote control signal and sensing information from sensors). In general, there might be a number of devices of low-data-rate applications to be connected to the AP. MTC [5]–[7] may belong to the second type, which is an important issue in next generation cellular systems. In this type of applications, coordinated multiple access schemes could suffer from a high control overhead including identifying active devices among devices within a system.

To reduce signaling and control overhead, random access (for uncoordinated multiple access) can be considered for MTC, where only a fraction of devices are active as in [2].

In [8]–[12], compressive random access schemes are studied using the notion of compressive sensing (CS) [13]–[16], which allows low-complexity multiple signal detection at an AP. Since the AP needs to know the channel state information (CSI) for multiple signal detection, each active device has to transmit a pilot signal for the CSI estimation at the AP. In random access, since multiple devices can transmit signals simultaneously, pilot signals should be different so that an AP can perform joint channel estimation to estimate the CSI of each active device. In [6], an active device is to randomly choose a preamble from a set of predetermined preambles for random access. In [17]–[19], based on the approach in [6], the CSI estimation[1] is considered for compressive random access over frequency-selective fading channels. In most cases, the device identification has to be carried out once connection is established as a separate step, which may result in additional signaling overhead. Thus, when devices transmit short packets, it would be beneficial if device identification can be carried out without any additional step to send a device identification sequence.

In this paper, we consider compressive random access that allows the AP to perform the CSI estimation as well as joint device identification with data detection. The main advantage of the proposed approach over those in [17]–[19] is that the active device identification can be carried out without any separate step. Since the proposed approach has a low signaling/control overhead, it would be attractive to the case of many devices of short data packets (few bytes) with low activity (i.e., the number of active devices would be a fraction of the devices in a system).

The main contributions of this paper are as follows.

1) A random access scheme is proposed to allow an AP to estimate the CSI of active devices as well as identify active devices with unique identification sequences with low signaling/control overhead.
2) A low-complexity algorithm to perform joint active device identification and data detection is derived using the expectation and maximization (EM) algorithm. Note that this paper is an extension of its conference version in [20] with new materials including the channel estimation and the EM-based active device identification (in Sections III and IV, respectively).

This paper is organized as follows. In Section II, we present the system model based on a multicarrier system over frequency selective fading channels and introduce the problem of active device identification for a system of many devices when a fraction of them are active. In Section III, we explain a two-stage transmission approach for the channel estimation and active device identification in detail. In Section IV, we derive computationally efficient methods to estimate the channels of active devices in stage I and to perform joint identification and detection in stage II using a well-known sparse signal estimation method. We present simulation results in Section V and conclude this paper with some remarks in Section VI.

[1]Note that in [8], [9], [11], and [12], no CSI is considered, while in [10] the CSI estimation is studied for flat-fading channels.

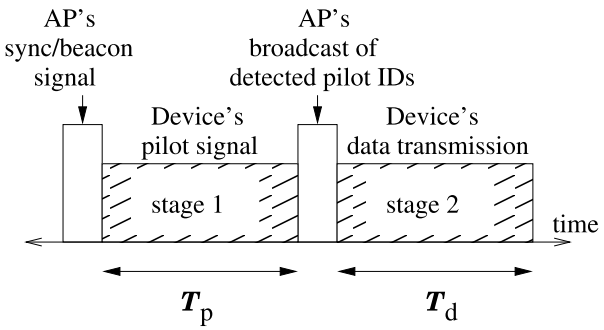

Fig. 2. Illustration of two-stage (uplink) access scheme with the AP's synchronous signal that initiates uplink access by devices.

II. System Model

Throughout this paper, we consider a single-cell with an AP and K devices as shown in Fig. 1 and multicarrier uplink transmissions with L subcarriers. It is assumed that $K \gg L$, while only a fraction of devices become active to transmit their signals to the AP or gateway. For convenience, we denote by M the number of active devices and assume that $M < L$. In addition, denote by $\mathcal{A}$ the index set of active devices. Clearly, we have $|\mathcal{A}| = M$, where $|\mathcal{A}|$ denotes the cardinality of set $\mathcal{A}$. It is also assumed that each device has a unique identification sequence. Since we consider a large K per cell (for a multicell system consisting of multiple cells, there should be a number of identification sequences, say more than 10^6), there should be a sufficient number of identification sequences for devices.

A. System Model for Two-Stage Access Scheme

In this section, we present the system model for a two-stage uplink access scheme that is illustrated in Fig. 2. At the beginning of a slot, the AP broadcasts a synchronous (or beacon) signal. Then, in stage I, the devices transmit uplink pilot signals to the AP so that the AP can estimate the channels for the (coherent) detection of the signals from devices at the AP. In order to have a low overhead for the channel estimation, we assume that only active devices can send pilot signals that are chosen randomly from a codebook of pilot signals, which is predefined and common to all devices. The pilot signaling in stage I is similar to that in [6]. In Section III-A, we derive a CS-based joint channel estimation method for stage I.

In stage II, active devices transmit their signals with unique identification sequences. Since the AP has CSI, it can perform coherent detection to not only detect data symbols, but also identify active devices. We devise a method for joint active device identification and data detection in Section III-B.

We now consider the received signal at the AP. Let $r_{l,t}$ denote the received signal at the AP through subcarrier l during time t. Then, it can be shown that

$$\begin{aligned}\mathbf{r}_t &= \begin{bmatrix} r_{0,t} & \dots & r_{L-1,t} \end{bmatrix}^{\mathrm{T}} \\ &= \sum_{k \in \mathcal{A}} \mathbf{H}_{k,t}\mathbf{a}_{k,t} + \mathbf{n}_t, \ t \in \mathcal{T}_p, \ t \in \mathcal{T}_d \end{aligned} \tag{1}$$

where the superscript T (H, resp.) stands for the transpose (the Hermitian transpose, resp.), $\mathbf{n}_t = [n_{0,t} \ \dots \ n_{L-1,t}]^{\mathrm{T}} \sim \mathcal{CN}(0, N_0\mathbf{I})$ is the background noise, and $\mathbf{H}_{k,t}$ and $\mathbf{a}_{k,t}$ are

the channel matrix and transmitted signals from device $k \in \mathcal{A}$, respectively. Here, $\mathcal{CN}(\mathbf{a}, \mathbf{R})$ ($\mathcal{N}(\mathbf{a}, \mathbf{R})$, resp.) represents the distribution of circularly symmetric complex Gaussian (CSCG) (real-valued Gaussian, resp.) random vectors with mean vector $\mathbf{a}$ and covariance matrix $\mathbf{R}$. In addition, $\mathcal{T}_p$ and $\mathcal{T}_\mathrm{d}$ represent the sets of time indices for the pilot transmission in stage I and the data transmission in stage II, respectively, as shown in Fig. 2. Throughout this paper, we assume that

$$\mathbf{H}_{k,t} = \mathbf{H}_k, \ \ t \in \mathcal{T}_p, \ \ t \in \mathcal{T}_d$$

which means that the time duration for stages I and II is less than or equal to the coherence time, and $\mathbf{H}_k$ is given by

$$\mathbf{H}_k = \mathrm{diag}\big(H_{k,0}, \ldots, H_{k,L-1}\big) \tag{2}$$

where $\mathrm{diag}(a_1, \ldots, a_L)$ denotes the diagonal matrix with the diagonal elements, $a_1, \ldots, a_L$, and

$$H_{k,l} = \sum_{i=0}^{P_k-1} h_{k,i} e^{-j\frac{2\pi il}{L}}, \ \ l = 0, \ldots, L-1.$$

Here, $\{h_{k,i}\}$ is the (uplink) channel impulse response (CIR) from device k to the AP and P_k is the length of CIR. For convenience, we assume that $P_k = P$ for all k.

B. CDMA for Identification

For active device identification, we may consider an additional step prior to data transmissions using unicast communication for each active device as in [21]. However, in order to efficiently exploit radio resources, it would be desirable to identify active devices simultaneously (not by unicast communication). To this end, we may consider multicarrier CDMA (MC-CDMA) with a unique spreading code for each device.

In order to focus on the identification of active devices, we now assume that the AP knows[2] the channel matrices of all devices, $\{\mathbf{H}_k\}$. Note that if the channel matrices, $\{\mathbf{H}_k\}$, are different and known to the AP, they can be used as signatures to identify active devices. However, as the channel matrices are random and vary, it may not be easy to use them as signatures. Thus, in this paper, we assume that each device has a unique sequence for identification purposes.

Let $\mathbf{c}_k$ be the unique spreading code for device k. Then, $\mathbf{a}_{k,t}$ can be written as

$$\mathbf{a}_{k,t} = \mathbf{c}_k d_{k,t} \tag{3}$$

where $d_{k,t} \in \mathcal{D}$ is the data symbol from device k. Here, $\mathcal{D}$ is the signal alphabet and $d_{k,t}$ is assumed to be independent. For simplicity, we assume that $\mathcal{D} = \{-1, +1\}$ (i.e., binary phase shift keying is used) throughput this paper. This approach is referred to as the MC-CDMA-based approach. A salient feature of the MC-CDMA-based approach is that the transmissions of identification sequences and data symbols of active devices can be carried out simultaneously. In [22] and [23], the identification of active users is studied when a fraction of users are active. If the number of bits to be transmitted from active devices is not large, this approach can efficiently exploit limited radio resources. In [9] and [12], exploiting the sparsity of active devices, CS-based approaches to estimate sparse signals are considered for the identification of active devices as well as the detection of their signals (in [9], the CDMA system with the sparsity of active devices is referred to as sparse CDMA).

Throughout this paper, we denote by N_I the number of all the possible unique identification sequences for a system that may consist of multiple cells (where there is one AP in a cell). Clearly, we need $N_I \gg K$. In the MC-CDMA-based approach, if $[\mathbf{c}_k]_l \in \{-1, +1\}$ (i.e., binary spreading codes), there could be $N_I = 2^{L-1}$ possible spreading codes [a pair of symmetric sequences, $(\mathbf{c}_k, -\mathbf{c}_k)$, is considered as the same one to avoid the ambiguity due to $\mathcal{D} = \{-1, +1\}$]. In general, since the number of possible sequences, N_I, grows exponentially with L, this approach might be suitable for the case of many devices. For example, if $L = 64$, we can provide unique identification sequences to up to $N_I = 2^{63} \approx 9 \times 10^{18}$ devices in a system.

C. Computational Complexity of Device Identification

In this section, we consider the computational complexity of device identification when each device has a unique $\mathbf{c}_k$. For convenience, we omit the time index t in this section.

At the AP, in order to identify the active devices and detect their data symbols, the maximum likelihood (ML) approach (with known $\{\mathbf{H}_k\}$) can be considered as follows:

$$\begin{aligned}\left\{\hat{\mathcal{A}}, \hat{\mathbf{d}}\right\} &= \underset{\mathcal{A},\mathbf{d}}{\mathrm{argmax}} f(\mathbf{r} \mid \{\mathbf{H}_k\}, \{\mathbf{c}_k\}, \{d_k\}, k \in \mathcal{A}) \\ &= \underset{\mathcal{A},\mathbf{d}}{\mathrm{argmin}} \left\| \mathbf{r} - \sum_{k \in \mathcal{A}} \mathbf{H}_k \mathbf{c}_k d_k \right\|_2^2 \end{aligned} \tag{4}$$

where $f(\mathbf{r} \mid \{\mathbf{H}_k\}, \{\mathbf{c}_k\}, \{d_k\}, k \in \mathcal{A})$ is the likelihood function of $\mathcal{A}$ and $\{d_k\}$ for given $\mathbf{r}$, $\mathbf{d} = \{d_k, k \in \mathcal{A}\}$, and $\|\mathbf{a}\|_p$ denotes the p-norm of vector $\mathbf{a}$ (note that if $p = 2$, the norm will be simply denoted by $\|\mathbf{a}\|$ without the subscript). If we only consider the identification of active devices in stage II, active devices can transmit known signals. In this case, since $\mathbf{d}$ is known, the ML approach in (4) is to determine $\mathcal{A}$.

Unfortunately, there is a serious drawback of the ML approach in (4). This ML approach becomes computationally infeasible for a large number of devices. To see this, we can consider the number of the possible $\mathcal{A}$'s, which is given by

$$N_\mathcal{A} = \binom{K}{M} \le \binom{N_I}{M}. \tag{5}$$

For relative small numbers of K and M, say $K = 100$ and $M = 5$, we have $N_\mathcal{A} \approx 75 \times 10^6$. Thus, if an exhaustive search is used, the ML approach in (4) is computationally prohibitive.

Note that in (5), the upper-bound might be valid if the AP does not know the identification sequences of K devices within the system in advance. Furthermore, if the number of active devices, M, is not known, the computational complexity of the ML approach would be even higher.

[2]This assumption is not realistic if K is large as the overhead for the channel estimation for all the K devices is significant. An efficient approach for the channel estimation will be discussed in Section III.

III. Two-Stage Transmissions and CS-Based Estimation and Identification

In Section II, we assume that the AP has full CSI in the active device identification. The channel estimation can be carried out at the AP in stage I when the devices transmit uplink pilot signals as shown in Fig. 2. If the AP is to know full CSI, the overhead of the channel estimation becomes significant when K is large. In fact, since the AP only needs to know the CSI of active devices, it is possible to reduce the overhead of uplink pilot signaling, which is the main issue in Section III-A. We also derive a low-complexity approach for the active device identification during stage II in Section III-B to overcome the difficulty discussed in Section II-C.

A. Stage I: Channel Estimation

Suppose that there is a codebook of D pilot spreading sequences for the uplink training to estimate the CSI of active devices, which are denoted by $\{\mathbf{p}_i,\ i = 1, \ldots, D\}$. Each device can choose one of the pilot sequences in the codebook randomly. Let $i(k)$ denote the pilot spreading sequence that is chosen by device $k \in \mathcal{A}$. In addition, let $\mathbf{x} = \mathbf{r}_t$, $t \in \mathcal{T}_p$, which is the received signal at the AP in stage I. Then, we have

$$\begin{aligned}\mathbf{x} &= \sum_{k\in\mathcal{A}} \mathbf{H}_k \mathbf{p}_{i(k)} + \mathbf{n}_{\mathrm{p}} \\ &= \sum_{k\in\mathcal{A}} \mathrm{diag}\big(\mathbf{p}_{i(k)}\big)\mathbf{F}\mathbf{h}_k + \mathbf{n}_{\mathrm{p}} \end{aligned} \tag{6}$$

where $[\mathbf{F}]_{l,p} = e^{-(j2\pi lp/L)}$, $l \in \{0, \ldots, L-1\}$, $p \in \{0, \ldots, P-1\}$, $\mathbf{h}_k = [h_{k,0}\ \ldots\ h_{k,P-1}]^{\mathrm{T}}$, and $\mathbf{n}_p \sim \mathcal{CN}(0, N_0\mathbf{I})$ is the background noise vector. Let $\mathbf{P}_i = \mathrm{diag}(\mathbf{p}_i)$. Then, we have

$$\begin{aligned}\mathbf{x} &= \underbrace{[(\mathbf{P}_1\mathbf{F})\ \ldots (\mathbf{P}_D\mathbf{F})]}_{=\bar{\mathbf{P}}} \begin{bmatrix}\mathbf{e}_1 \\ \vdots \\ \mathbf{e}_D\end{bmatrix} + \mathbf{n}_{\mathrm{p}} \\ &= \bar{\mathbf{P}}\mathbf{e} + \mathbf{n}_{\mathrm{p}} \end{aligned} \tag{7}$$

where

$$\mathbf{e}_i = \sum_{k\in\mathcal{C}_i} \mathbf{h}_{i(k)}. \tag{8}$$

and $\mathbf{e} = [\mathbf{e}_1^{\mathrm{T}}\ \ldots\ \mathbf{e}_D^{\mathrm{T}}]^{\mathrm{T}}$. Here, $\mathcal{C}_i$ is the index set of the active devices that choose $\mathbf{p}_i$. Thus, $|\cup_{i=1}^{D} \mathcal{C}_i| = M$ and $\mathcal{C}_i \cap \mathcal{C}_m = \emptyset$ for $i \neq m$.

Since the number of active devices is M, there might be at most MP nonzero elements in $\mathbf{e}$. Note that $\mathbf{e}$ is a DP $\times$ 1 vector, while the size of $\bar{\mathbf{P}}$ in (7) is $L \times$ DP. From this, the estimate of $\mathbf{e}$ can be found as

$$\hat{\mathbf{e}} = \underset{\mathbf{e}\in\Sigma_{\mathrm{MP}}}{\mathrm{argmin}} \big\|\bar{\mathbf{P}}\mathbf{e} - \mathbf{x}\big\|^2. \tag{9}$$

This minimization is computational infeasible when L and D are large. However, since $\mathbf{e}$ can be seen as a sparse signal when $M \ll D$, we could use CS-based sparse signal estimation approaches to estimate $\mathbf{e}$, which is discussed in Section IV.

The estimate of $\mathbf{e}$ from (7) can only provide the CSI of active devices. This CSI will be used to identify active devices in the second stage. We assume that the AP can detect M used pilot spreading sequences in the first stage (thus, there are at least M active devices). For convenience, the M estimated channel matrices are denoted by $\bar{\mathbf{H}}_m$, $m = 0, \ldots, M-1$. Once $\{\bar{\mathbf{H}}_m\}$ is available, in the second stage, the AP could identify the active devices and their data symbols.

There could be multiple active devices that choose the same pilot spreading sequence from the codebook, say the ith pilot spreading sequence. In this case, $\mathbf{e}_i$ is a superposition of the CIRs of the active devices that choose the ith pilot spreading sequence as in (8), i.e., $|\mathcal{C}_i| > 1$, and the AP fails to estimate the CSI for those active devices. This event is referred to as the pilot collision. Furthermore, although there is no pilot collision, the AP may also fail to estimate some active devices' channels due to various reasons. If some of chosen pilot spreading sequences are highly correlated, the AP may fail to estimate $\mathbf{e}$ in the presence of the background noise. Thus, it is important to design a good codebook of pilot spreading sequences. In this paper, however, we do not consider this issue as it is beyond the scope of this paper.

B. Stage II: Device Identification and Signal Detection

As illustrated in Fig. 2, after stage I, the AP can broadcast the pilot IDs that are not collided. Thus, in stage II, we assume that the active devices that do not have any pilot collisions can transmit their signals with unique identification sequences.

In this paper, we propose to use sparse $\mathbf{c}_k$ based on the index modulation [24], [25] for active device identification. Suppose that each device can use a subset of subcarriers to transmit its signal and $\mathbf{c}_k$ is sparse. Denote by Q the number of nonzero elements of $\mathbf{c}_k$. Then, the number of all possible identification sequences becomes $N_I = \binom{L}{Q}$. Let $p = Q/L$. From [26], we can have the following lower-bound on N_I:

$$N_I \geq \frac{1}{\sqrt{8Lp(1-p)}} 2^{LH_b(p)} \tag{10}$$

where $H_b(p) = -p\log_2 p - (1-p)\log_2(1-p)$. For a fixed p, we can see that the number of identification sequences can grow exponentially with L. Furthermore, noting that $\mathbf{a}_k$ is a complex-valued vector, we can consider a Q-sparse $2L \times 1$ real-valued vector for $\mathbf{a}_k$, which can further increase N_I. To see this, we can rewrite (1) as

$$\begin{bmatrix}\Re(\mathbf{r}) \\ \Im(\mathbf{r})\end{bmatrix} = \sum_{k\in\mathcal{A}} \tilde{\mathbf{H}}_k \tilde{\mathbf{a}}_k + \begin{bmatrix}\Re(\mathbf{n}) \\ \Im(\mathbf{n})\end{bmatrix} \tag{11}$$

where

$$\tilde{\mathbf{H}}_k = \begin{bmatrix}\Re(\mathbf{H}_k) & -\Im(\mathbf{H}_k) \\ \Im(\mathbf{H}_k) & \Re(\mathbf{H}_k)\end{bmatrix} \text{ and } \tilde{\mathbf{a}}_k = \begin{bmatrix}\Re(\mathbf{a}_k) \\ \Im(\mathbf{a}_k)\end{bmatrix}.$$

For convenience, we denote by $\tilde{\mathbf{x}}$ the real-valued version of a complex-valued vector $\mathbf{x}$ throughout this paper. Since $d_k \in \{-1, +1\}$ is real-valued, we have

$$\tilde{\mathbf{a}}_k = \tilde{\mathbf{c}}_k d_k$$

where $\tilde{\mathbf{c}}_k = \begin{bmatrix}\Re(\mathbf{c}_k) \\ \Im(\mathbf{c}_k)\end{bmatrix}$. In this case, N_I becomes

$$N_I = \binom{2L}{Q}.$$

The resulting approach is referred to as the sparse index multiple access (SIMA)-based approach.

For example, if $L = 64$ and $Q = 5$, we have $N_I \approx 7.6 \times 10^6$. Therefore, the SIMA-based approach that uses sparse $\mathbf{c}_k$ can generate a sufficiently large number of identification sequences for devices in a system, although N_I is much smaller than that in the CDMA-based approach, which is $2^{L-1} \approx 9 \times 10^{18}$ when $L = 64$.

The conventional index modulation approach may suffer from frequency-selective fading [27], since only few subcarriers are used by each device to access the uplink channel. In particular, if the selected subcarriers by a device experience severe fading, the AP may have difficulties to detect the signal from this device. To mitigate this problem, precoding [28], [29] can be used as in [27]. Let $\mathbf{W}$ denote the complex-valued precoding matrix of size $L \times L$. We assume that this precoding matrix, $\mathbf{W}$, is used by all devices to mitigate frequency-selective fading as mentioned earlier. Throughout this paper, we assume that $\mathbf{W}$ is a unitary matrix of nonzero elements. Let

$$\tilde{\mathbf{W}} = \begin{bmatrix} \Re(\mathbf{W}) & -\Im(\mathbf{W}) \\ \Im(\mathbf{W}) & \Re(\mathbf{W}) \end{bmatrix} = \begin{bmatrix} \tilde{\mathbf{w}}_1 & \dots & \tilde{\mathbf{w}}_{2L} \end{bmatrix}.$$

Then, $\tilde{\mathbf{c}}_k$ is given by

$$\tilde{\mathbf{c}}_k = \sum_{i \in I_k} \tilde{\mathbf{w}}_i = \tilde{\mathbf{W}} \tilde{\mathbf{u}}_k, \ k = 0, \dots, K-1 \tag{12}$$

where I_k is the unique index set for device k, which is used for the device identification, and $\tilde{\mathbf{u}}_k$ of size $2L \times 1$ is

$$[\tilde{\mathbf{u}}_k]_i = \begin{cases} \frac{1}{\sqrt{Q}}, & \text{if } i \in I_k \\ 0, & \text{otherwise.} \end{cases} \tag{13}$$

For SIMA, we assume that $|I_k| = Q$. Note that $\|\tilde{\mathbf{u}}_k\| = 1$ for normalization purposes. In (12), $\tilde{\mathbf{c}}_k$ is not sparse, but $\tilde{\mathbf{u}}_k$, which is Q-sparse. For convenience, $\tilde{\mathbf{u}}_k$ is referred to as the sparse identification vector (SIV) for device k. For convenience, denote by $\tilde{\mathcal{U}}$ the set of the Q-sparse SIVs of size $2L \times 1$ that are defined as in (13). Note that $\mathbf{c}_k = \mathbf{W}\mathbf{u}_k$ if we define $\mathbf{u}_k$ as

$$\mathbf{u}_k = \tilde{\mathbf{u}}_{1:L} + j\tilde{\mathbf{u}}_{L+1:2L}.$$

For convenience, let

$$\mathcal{U} = \left\{ \mathbf{u} | \mathbf{u} = \tilde{\mathbf{u}}_{1:L} + j\tilde{\mathbf{u}}_{L+1:2L}, \ \tilde{\mathbf{u}} \in \tilde{\mathcal{U}} \right\}. \tag{14}$$

Then, $\mathbf{u}_k \in \mathcal{U}$, while $\tilde{\mathbf{u}}_k \in \tilde{\mathcal{U}}$.

Denote by $\mathbf{v}_m \in \mathcal{U}$ the SIV used by the active device associated with the channel matrix $\bar{\mathbf{H}}_m$ that is estimated in stage I. For convenience, denote by $\tilde{\mathbf{v}}_m \in \tilde{\mathcal{U}}$ the real-valued version of $\mathbf{v}_m$. Note that $\mathbf{u}_k \in \mathcal{U}$ is the unique SIV for device k, while $\mathbf{v}_m \in \mathcal{U}$ is the SIV of the active device that is associated with $\bar{\mathbf{H}}_m$ in stage I. In stage II, with known $\bar{\mathbf{H}}_m$, the AP can perform coherent detection to decide $\mathbf{v}_m$ as will be shown below. Once $\mathbf{v}_m$ is known, the AP can identify the active device associated with $\bar{\mathbf{H}}_m$ by finding the index $k(m)$ such that $\mathbf{u}_{k(m)} = \mathbf{v}_m$.

Consider $\mathbf{r}_t$, $t \in \mathcal{T}_\mathrm{d}$ in stage II. For convenience, we omit the time index t. Then, we have

$$\begin{aligned} \mathbf{r} &= \sum_{k \in \mathcal{A}} \mathbf{H}_k \mathbf{a}_k + \mathbf{n} \\ &= \begin{bmatrix} (\bar{\mathbf{H}}_0 \mathbf{W}) & \dots & (\bar{\mathbf{H}}_{M-1} \mathbf{W}) \end{bmatrix} \begin{bmatrix} \mathbf{v}_0 \bar{d}_0 \\ \vdots \\ \mathbf{v}_{M-1} \bar{d}_{M-1} \end{bmatrix} + \mathbf{n} \end{aligned} \tag{15}$$

where $\bar{d}_m \in \mathcal{D}$ represents the data symbol that is transmitted by the active device associated with the channel matrix $\bar{\mathbf{H}}_m$. Letting

$$\mathbf{G}_m = \begin{bmatrix} \Re(\bar{\mathbf{H}}_m \mathbf{W}) & -\Im(\bar{\mathbf{H}}_m \mathbf{W}) \\ \Im(\bar{\mathbf{H}}_m \mathbf{W}) & \Re(\bar{\mathbf{H}}_m \mathbf{W}) \end{bmatrix}$$

it can be shown that

$$\mathbf{r} = \begin{bmatrix} \Re(\mathbf{r}) \\ \Im(\mathbf{r}) \end{bmatrix} = \mathbf{G}\mathbf{b} + \tilde{\mathbf{n}} \tag{16}$$

where $\tilde{\mathbf{n}} = \begin{bmatrix} \Re(\mathbf{n}) \\ \Im(\mathbf{n}) \end{bmatrix}$, $\mathbf{G} = [\mathbf{G}_0 \ \dots \ \mathbf{G}_{M-1}]$ is the second-stage measurement matrix of size $2L \times 2LM$, and

$$\mathbf{b} = \begin{bmatrix} (\tilde{\mathbf{v}}_0 \bar{d}_0)^\mathrm{T} & \dots & (\tilde{\mathbf{v}}_{M-1} \bar{d}_{M-1})^\mathrm{T} \end{bmatrix}^\mathrm{T}.$$

Note that since $\tilde{\mathbf{v}}_m \in \tilde{\mathcal{U}}$ is a Q-sparse signal, $\bar{\mathbf{b}}$ of size $2LM \times 1$ in (16) is an MQ-sparse vector. Since the measurement matrix, $\mathbf{G}$, in (16) is available at the AP from stage I, an estimate of $\mathbf{b}$ can be found as

$$\hat{\mathbf{b}} = \underset{\mathbf{b} \in \Sigma_{MQ}}{\operatorname{argmin}} \|\mathbf{r} - \mathbf{G}\mathbf{b}\|^2. \tag{17}$$

Once $\mathbf{b}$ is estimated, the data symbols, $\bar{d}_m$'s, and the SIVs, $\tilde{\mathbf{v}}_m$'s, can be found from $\hat{\mathbf{b}}$. This shows that the identification of active devices can be carried out by estimating the sparse vector $\mathbf{b}$ in (17) using a low-complexity CS estimation method. That is, the computational complexity for the identification of active devices can be much lower than that of the ML approach in (4). For example, suppose that the orthogonal matching pursuit (OMP) algorithm [30], [31], which is one of the greedy algorithms for sparse signal estimation, is used. The complexity of the OMP algorithm depends on the size of the measurement matrix and the sparsity [16, Ch. 8]. In (17), since the size of $\mathbf{G}$ is $2L \times 2LM$ and $\mathbf{b}$ is MQ-sparse, the complexity of the OMP algorithm to find an approximate solution to the problem in (17) becomes $O(LMQ)$, which is clearly much lower than that for the ML approach in (4).

IV. CS-Based Estimation for Stages I and II

In this section, we derive low-complexity estimation methods to solve the problems in (9) and (17) for stages I and II, respectively, based on the OMP algorithm.

A. Modified OMP Algorithm for Channel Estimation

Among various approaches to estimate sparse signals, we consider the OMP algorithm [30], [31] to estimate $\mathbf{e}$ in (7), which is an MP-sparse signal, or find an approximate solution to (9) for the channel estimation in stage I. We can summarize the conventional OMP algorithm from [16, Ch. 8] as in Algorithm 1.

Here, the superscript † denotes the pseudo-inverse and for a matrix $\mathbf{X}$ (a vector $\mathbf{a}$, resp.), $[\mathbf{X}]_n$ ($[\mathbf{a}]_n$, resp.) represents the nth column (element, resp.). If n is a set of indices, $[\mathbf{X}]_n$ is a submatrix of $\mathbf{X}$ obtained by taking the corresponding columns.

Since the conventional OMP algorithm does not take into account the structure of $\mathbf{e}$, we can modify it for a better performance. As shown in (8), $\mathbf{e}$ is block-sparse. That is, $\mathbf{e}_i$ is either a zero or nonzero vector. To take into account this structure, we can modify the OMP algorithm as in Algorithm 2.

Algorithm 1 Conventional OMP Algorithm

*) Inputs: $\mathbf{x}$, $\mathbf{\Phi} = \bar{\mathbf{P}}$, and $S = MP$
0) Initialize: $\boldsymbol{\zeta}_{(0)} = \mathbf{x}$, $\mathbf{e}_{(0)} = \mathbf{0}$, and $\mathcal{T}_{(0)} = \emptyset$
1) for $i = 1 : S$
2) $\quad \boldsymbol{\beta}_{(i)} = \mathbf{\Phi}^{\mathrm{T}} \boldsymbol{\zeta}_{(i-1)}$
3) $\quad p^* = \operatorname{argmax}_p \frac{|[\boldsymbol{\beta}_{(i)}]_p|}{\|[\mathbf{\Phi}]_p\|}$
4) $\quad \mathcal{T}_{(i)} = \mathcal{T}_{(i-1)} \cup p^*$
5) $\quad [\mathbf{e}_{(i)}]_{\mathcal{T}} = [\mathbf{\Phi}_{\mathcal{T}_{(i)}}]^{\dagger} \mathbf{x}$
6) $\quad \boldsymbol{\zeta}_{(i)} = \mathbf{x} - \mathbf{\Phi} \mathbf{e}_{(i)}$
7) end;
8) Outputs: $\boldsymbol{\zeta}_{(i)}$ and $\hat{\mathbf{e}} = \mathbf{e}_{(S)}$.

Algorithm 2 Block OMP Algorithm

*) Inputs: $\mathbf{x}$, $\mathbf{\Phi} = \bar{\mathbf{P}}$, M, and P
0) Initialize: $\boldsymbol{\zeta}_{(0)} = \mathbf{x}$, $\mathbf{e}_{(0)} = \mathbf{0}$, and $\mathcal{T}_{(0)} = \emptyset$
1) for $i = 1 : M$
2) $\quad \boldsymbol{\beta}_{(i)} = \mathbf{\Phi}^{H} \boldsymbol{\zeta}_{(i-1)}$
3) $\quad p^* = \operatorname{argmax}_p \sum_{q=(p-1)P+1}^{pP} |\frac{[\boldsymbol{\beta}_{(i)}]_q}{\|[\mathbf{\Phi}]_q\|}|$
4) $\quad \mathcal{T}_{(i)} = \mathcal{T}_{(i-1)} \cup \{(p^*-1)P + 1, \ldots, p^*P\}$
5) $\quad [\mathbf{e}_{(i)}]_{\mathcal{T}} = [\mathbf{\Phi}_{\mathcal{T}_{(i)}}]^{\dagger} \mathbf{x}$
6) $\quad \boldsymbol{\zeta}_{(i)} = \mathbf{x} - \mathbf{\Phi} \mathbf{e}_{(i)}$
7) end;
8) Outputs: $\boldsymbol{\zeta}_{(i)}$ and $\hat{\mathbf{e}} = \mathbf{e}_{(M)}$.

This modified OMP algorithm is referred to as the block-OMP algorithm in this paper. Note that the selection strategy in line 3 is an example to take into account the block-sparsity of $\mathbf{e}$ based on the 1-norm. There are other selection strategies to choose the index or atom, which need to be studied as a further research topic.

B. EM Algorithm for Joint Identification and Detection

In this section, we consider the joint active device identification and data detection when active devices transmit sequences of data symbols in stage II using the EM algorithm [32], [33].

Let $\mathcal{T}_{\mathrm{d}} = \{0, \ldots, T-1\}$, i.e., the number of data symbols in stage II is T. Then, from (16), the received signal at the tth symbol transmission in stage II is given by

$$\mathbf{r}_t = \mathbf{G}\mathbf{B}_t\mathbf{z} + \tilde{\mathbf{n}}_t, \;\; t = 0, \ldots, T-1 \tag{18}$$

where $\mathbf{B}_t = \operatorname{diag}(\bar{d}_{0,t} \;\ldots\; \bar{d}_{M-1,t}) \otimes \mathbf{I}$ and $\mathbf{z} = [\tilde{\mathbf{v}}_0^{\mathrm{T}} \;\ldots\; \tilde{\mathbf{v}}_{M-1}^{\mathrm{T}}]^{\mathrm{T}}$. Here, $\otimes$ denotes the Kronecker product and $\bar{d}_{m,t}$ is the tth data symbol transmitted by the active device associated with the channel matrix $\bar{\mathbf{H}}_m$ and $\tilde{\mathbf{n}}_t \sim \mathcal{N}(0, [N_0/2]\mathbf{I})$ is an independent background noise. It is noteworthy that since each device has a unique identification sequence, $\tilde{\mathbf{v}}_m$ is invariant during T-symbol transmission in (18).

With all received signal vectors, under the ML criterion, we have the following joint identification and detection problem:

$$\begin{aligned}\left\{\hat{\mathbf{z}}, \hat{\mathbf{B}}\right\} &= \operatorname*{argmax}_{\mathbf{z},\mathbf{B}} \prod_{t=0}^{T-1} f(\mathbf{r}_t|\mathbf{z}, \mathbf{B}_t) \\ &= \operatorname*{argmax}_{\mathbf{z},\mathbf{B}} \prod_{t=0}^{T-1} \exp\left(-\frac{2}{N_0}\|\mathbf{r}_t - \mathbf{G}\mathbf{B}_t\mathbf{z}\|^2\right) \\ &= \operatorname*{argmin}_{\mathbf{z},\mathbf{B}} \sum_{t=0}^{T-1} \|\mathbf{r}_t - \mathbf{G}\mathbf{B}_t\mathbf{z}\|^2 \end{aligned} \tag{19}$$

where $f(\mathbf{r}_t|\mathbf{z}, \mathbf{B}_t)$ is the likelihood function for given $\mathbf{r}_t$ and $\mathbf{B} = [\mathbf{B}_0 \;\ldots\; \mathbf{B}_{T-1}]$, and proper constraints should be imposed on $\mathbf{z}$ and $\mathbf{B}$ (e.g., $\mathbf{z} \in \Sigma_{MQ}$). An exhaustive search to solve the problem in (19) is computationally infeasible. Thus, we may resort to the EM algorithm [32], [33].

For the EM algorithm, we consider the ML approach to estimate $\mathbf{z}$ as follows:

$$\hat{\mathbf{z}} = \operatorname*{argmax}_{\mathbf{z} \in \Sigma_{MQ}} \prod_{t=0}^{T-1} f(\mathbf{r}_t|\mathbf{z}) \tag{20}$$

where $f(\mathbf{r}_t|\mathbf{z})$ is the likelihood function of $\mathbf{z}$ for given $\mathbf{r}_t$. Taking $\mathbf{B}$ as the missing data (i.e., $\{\mathbf{r}_t, \mathbf{B}_t\}$ is considered the complete data, while $\{\mathbf{r}_t\}$ is the incomplete data), we can derive the EM algorithm, which is an iterative algorithm and consists of the E-step and M-step.

The E-step is given by

$$Q\left(\mathbf{z} \,|\, \hat{\mathbf{z}}^{(q)}\right) = \mathbb{E}_{\mathbf{B}}\left[\sum_{t=0}^{T-1} \|\mathbf{r}_t - \mathbf{G}\mathbf{B}_t\mathbf{z}\|^2 \,\middle|\, \{\mathbf{r}_t\}, \hat{\mathbf{z}}^{(q)}\right] \tag{21}$$

where $\hat{\mathbf{z}}^{(q)}$ denotes the estimate of $\mathbf{z}$ at the qth iteration and $\mathbb{E}_X[\cdot]$ represents the statistical expectation over random variable (or vector) X. Let

$$\begin{aligned}\mu_{m,t}^{(q)} &= \mathbb{E}\left[\bar{d}_{m,t} \,|\, \{\mathbf{r}_t\}, \hat{\mathbf{z}}^{(q)}\right] \\ \sigma_{m,t}^{(q)} &= \operatorname{Var}\left(\bar{d}_{m,t} \,|\, \{\mathbf{r}_t\}, \hat{\mathbf{z}}^{(q)}\right)\end{aligned} \tag{22}$$

where $\operatorname{Var}(\cdot)$ denotes the variance. Then, after some manipulations under the assumption that $\bar{d}_{m,t}$ is independent, it follows:

$$Q\left(\mathbf{z} \,|\, \hat{\mathbf{z}}^{(q)}\right) = \left\|\mathbf{y} - \mathbf{A}^{(q)}\mathbf{z}\right\|^2 + \mathbf{z}^H \mathbf{\Delta}^{(q)} \mathbf{z} \tag{23}$$

where

$$\mathbf{y} = \left[\mathbf{r}_0^{\mathrm{T}} \;\cdots\; \mathbf{r}_{T-1}^{\mathrm{T}}\right]^{\mathrm{T}}$$

$$\mathbf{A}^{(q)} = \begin{bmatrix} \mathbf{G}_0\mu_{0,0}^{(q)} & \cdots & \mathbf{G}_{M-1}\mu_{M-1,0}^{(q)} \\ \vdots & \ddots & \vdots \\ \mathbf{G}_0\mu_{0,T-1}^{(q)} & \cdots & \mathbf{G}_{M-1}\mu_{M-1,T-1}^{(q)} \end{bmatrix}$$

$$\mathbf{\Delta}^{(q)} = \begin{bmatrix} \mathbf{G}_0^H\mathbf{G}_0\sigma_0^{(q)} & \cdots & \mathbf{0} \\ \vdots & \ddots & \vdots \\ \mathbf{0} & \cdots & \mathbf{G}_{M-1}^H\mathbf{G}_{M-1}\sigma_{M-1}^{(q)} \end{bmatrix}.$$

The M-step is given by

$$\begin{aligned}\hat{\mathbf{z}}^{(q+1)} &= \operatorname*{argmin}_{\mathbf{z} \in \Sigma_{MQ}} Q\left(\mathbf{z} \,|\, \hat{\mathbf{z}}^{(q)}\right) \\ &= \operatorname*{argmin}_{\mathbf{z} \in \Sigma_{MQ}} \left\|\mathbf{y} - \mathbf{A}^{(q)}\mathbf{z}\right\|^2 + \mathbf{z}^H \mathbf{\Delta}^{(q)} \mathbf{z}.\end{aligned} \tag{24}$$

Due to the sparsity constraint, i.e., $\mathbf{z} \in \Sigma_{MQ}$, it is not easy to perform the M-step to find $\hat{\mathbf{z}}^{(q+1)}$, although the cost function is quadratic in $\mathbf{z}$. We can resort to a low-complexity greedy algorithm to find an approximate solution to the problem in (24).

Algorithm 3 C-OMP Algorithm

*) Inputs: $\mathbf{y}$, $\mathbf{\Phi} = \bar{\mathbf{A}}^{(q)}$, and $\bar{M} = MQ$
0) Initialize: $\boldsymbol{\zeta}_{(0)} = \mathbf{y}$, $\mathbf{z}_{(0)} = \mathbf{0}$, and $\mathcal{T}_{(0)} = \emptyset$
1) for $i = 1 : \bar{M}$
2) $\quad \boldsymbol{\beta}_{(i)} = \mathbf{\Phi}^{\mathrm{T}} \boldsymbol{\zeta}_{(i-1)}$
3a) $p^* = \mathrm{argmax}_{p \in \mathcal{I}^{(i)}} \frac{|[\boldsymbol{\beta}^{(i)}]_p|}{\|[\mathbf{\Phi}]_p\|}$
3b) $m^* = \lceil \frac{p^*}{2L} \rceil$
3c) $\mathcal{T}_{m^*}^{(i)} = \mathcal{T}_{m^*}^{(i-1)} \cup p^*$
3d) $\mathcal{T}^{(i)} = \cup_m \mathcal{T}_m^{(i)}$
3e) If $|\mathcal{T}_{m^*}^{(i)}| = Q$, $\mathcal{I}^{(i)} = \mathcal{I}^{(i-1)} \setminus \{2L(m^*-1)+1, \ldots, 2Lm^*\}$.
4) $\quad \mathcal{T}_{(i)} = \mathcal{T}_{(i-1)} \cup p^*$
5) $\quad [\mathbf{z}_{(i)}]_{\mathcal{T}} = [\mathbf{\Phi}_{\mathcal{T}_{(i)}}]^{\dagger} \mathbf{y}$
6) $\quad \boldsymbol{\zeta}_{(i)} = \mathbf{y} - \mathbf{\Phi} \mathbf{z}_{(i)}$
7) end;
8) Outputs: $\boldsymbol{\zeta}_{(i)}$ and $\hat{\mathbf{z}}^{(q+1)} = \hat{\mathbf{z}}_{(\bar{M})}$.

Since

$$\left\| \mathbf{y} - \mathbf{A}^{(q)} \mathbf{z} \right\|^2 + \mathbf{z}^H \mathbf{\Delta}^{(q)} \mathbf{z} = \left\| \mathbf{y}_{\mathrm{ex}} - \bar{\mathbf{A}}^{(q)} \mathbf{z} \right\|^2 \tag{25}$$

where

$$\mathbf{y}_{\mathrm{ex}} = \left[\mathbf{y}^H \ \mathbf{0}_{1 \times L} \right]^H \text{ and } \bar{\mathbf{A}}^{(q)} = \begin{bmatrix} \mathbf{A}^{(q)} \\ \mathbf{\Delta}^{(q)} \end{bmatrix}$$

the M-step in (24) becomes

$$\hat{\mathbf{z}}^{(q+1)} = \underset{\mathbf{z} \in \Sigma_{MQ}}{\mathrm{argmin}} \left\| \mathbf{y}_{\mathrm{ex}} - \bar{\mathbf{A}}^{(q)} \mathbf{z} \right\|^2. \tag{26}$$

The standard OMP algorithm can be used to find an approximate solution for $\mathbf{z}$ in (26), which is an $\bar{M}$-sparse signal, where $\bar{M} = MQ$. However, a better performance can be obtained if we take into account a special property of $\mathbf{z}$. Since $\mathbf{z}$ is a concatenation of M Q-sparse signal blocks (i.e., the $\tilde{\mathbf{v}}_m$'s), each block is Q-sparse. Thus, the selection strategy in line 3 of Algorithm 1 for the conventional OMP algorithm needs to be modified to take into account this constraint. The resulting OMP algorithm will be referred to as the constrained OMP (C-OMP) algorithm for convenience.

Denote by $\mathcal{T}_m^{(i)}$ the index set of the selected subcarriers for the device associated with the channel matrix $\bar{\mathbf{H}}_m$ at the ith iteration. We assume that $\mathcal{T}_m^{(0)} = \emptyset$. It is clear that $|\mathcal{T}_m^{(i)}|$ cannot be greater than Q as each $\tilde{\mathbf{v}}_m$ is Q-sparse. Let $\mathcal{I}^{(i)}$ denote the column index of $\mathbf{\Phi}$ at the ith iteration with $\mathcal{I}^{(0)} = \{1, \ldots, 2LM\}$. Then, the C-OMP algorithm can be summarized in Algorithm 3.

V. Simulation Results

In this section, we present simulation results. For simulations, we assume Rayleigh multipath fading channels, where the channel coefficients, $h_{k,i}$, are independent CSCG random variables with mean zero and variance $(1/P)$, that is

$$h_{k,i} \sim \mathcal{CN}\left(0, \frac{1}{P}\right). \tag{27}$$

Here, we also note that the channel gain for each device is assumed to be normalized, i.e., $\sum_{i=0}^{P-1} \mathbb{E}[|h_{k,i}|^2] = 1$. Provided that the transmission rate is low for MTC, the number of paths may not be large. For simulations, we will consider[3] $P = 3$ as in [17].

In addition, we consider randomly generated binary sequences for the codebook of the pilot sequences, $\mathbf{p}_i$'s in stage I (note that in this case each element of $\mathbf{p}_i$ is either 1 or -1). In stage II, for the precoding matrix $\mathbf{W}$, we consider a randomly generated complex-valued unitary matrix for each run.

For the performance evaluation in each stage, we have different performance metrics. In stage I, we consider the normalized mean squared error (NMSE) of the estimated channel, which is defined as

$$\mathrm{NMSE} = \mathbb{E}\left[\frac{\left\| \hat{\mathbf{e}} - \mathbf{e} \right\|^2}{\|\mathbf{e}\|^2} \right].$$

In stage II, for a performance metric, we consider the probability of unsuccessful identification, which is the probability that the AP fails to identify *all M* active devices' SIVs. Note that even if the event of unsuccessful identification occurs, the AP may be able to identify some of active devices.

In stage I, from (6), ignoring the interfering signals from the other active devices, the signal-to-noise ratio (SNR) is defined as

$$\begin{aligned} \mathrm{SNR} &= \frac{\mathbb{E}\left[\left\| \mathbf{H}_k \mathbf{p}_{i(k)} \right\|^2 \right]}{\mathbb{E}\left[\left\| \mathbf{n}_p \right\|^2 \right]} \\ &= \frac{\mathbb{E}\left[\|\mathbf{F}\mathbf{h}_k\|^2 \right]}{LN_0} \\ &= \frac{L\mathbb{E}\left[\|\mathbf{h}_k\|^2 \right]}{LN_0} \\ &= \frac{1}{N_0} \end{aligned} \tag{28}$$

because $\mathbb{E}[\|\mathbf{h}_k\|^2] = 1$ from (27). In stage II, with $\mathcal{D} = \{-1, +1\}$, the SNR in (28) becomes E_b/N_0, where E_b denotes the bit energy.

A. Results for Stage I

In this section, we present simulation results for the channel estimation in stage I. For performance comparisons, we also consider the channel estimation approach in [17], which is a time-domain pilot-based channel estimation method. Thus, the main difference between the approach in this paper and that in [17] is the domain of the signals for the channel estimation. The approach in this paper is referred to as the frequency-domain approach as the received signals in the frequency-domain is used, while that in [17] is referred to as the time-domain approach.

Fig. 3 shows simulation results of the channel estimation for various values of SNR when $L = 64$, $D = 320$, $M = 6$, and $P = 3$. The NMSE in Fig. 3 is obtained only for the case of no pilot collision. We can see that the NMSE decreases with the SNR.

[3] As in LTE, if 15 kHz subcarrier is considered, the symbol rate becomes 960 K symbols per second when $L = 64$. In this case, the number of paths, P, becomes 3 when the maximum delay spread is less than 3.125 μs. (which might be a case of suburban environment).

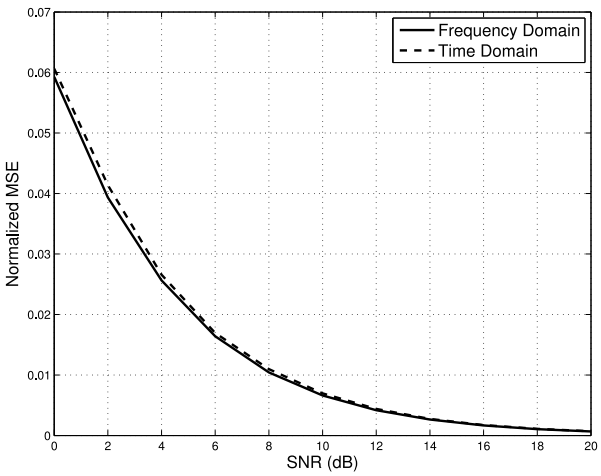

Fig. 3. NMSE of the estimated CSI in stage I for various SNRs when $L = 64$, $D = 320$, $M = 6$, and $P = 3$.

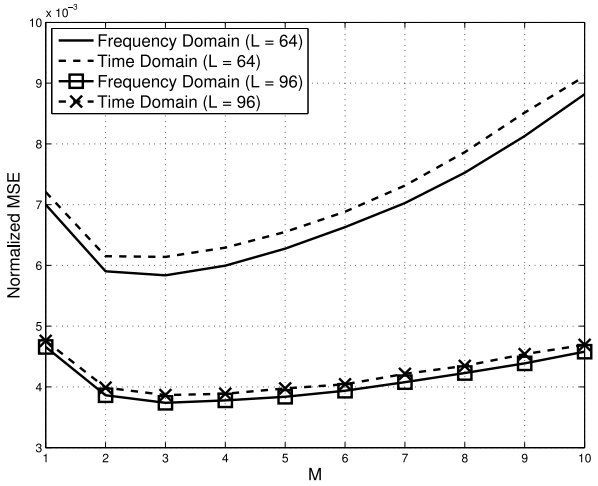

Fig. 5. NMSE of the estimated CSI in stage I for various values of M when $L \in \{64, 96\}$, $D = 320$, $P = 3$, and SNR $= 10$ dB.

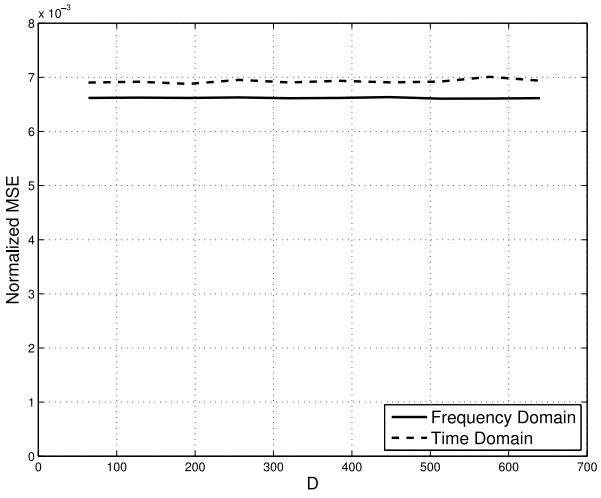

Fig. 4. NMSE of the estimated CSI in stage I for various values of D when $L = 64$, $M = 6$, $P = 3$, and SNR $= 10$ dB.

In Fig. 4, we show simulation results of the channel estimation for various sizes of the codebook of pilot sequences, D, when $L = 64$, $M = 6$, $P = 3$, and SNR $= 10$ dB. The NMSE of the estimated channel is almost independent of D.

Fig. 5 shows simulation results of the channel estimation for various numbers of active devices, M, when $L \in \{64, 96\}$, $D = 320$, $P = 3$, and SNR $= 10$ dB. It is shown that a better performance in terms of the NMSE can be obtained for a larger L.

From Figs. 3–5, we can observe that the frequency-domain approach (the approach in this paper) slightly outperforms the time-domain approach (that in [17]). Note that the frequency-domain approach needs to use the fast Fourier transform (FFT), which requires additional computational complexity compared to the time-domain approach. This might be a cost (which is a computational complexity of order $L \log_2 L$ for FFT) for a slightly better performance.

B. Results for Stage II

In this section, we present simulation results for the joint identification and detection using the EM algorithm derived in Section IV-B. With $T = 200$, we consider two types of CSI: 1) perfect CSI and 2) imperfect (or estimated) CSI. For imperfect CSI, we consider a fixed NMSE $= 0.05$ regardless of the SNR.

For comparison purposes, we consider the MC-CDMA-based approach with $K = L = 64$ and $M = 6$, which might be seen as a multicarrier version of the approaches in [17] and [18]. In the MC-CDMA-based approach, it is assumed that all the spreading sequences of $K = L$ devices in the system are known. It is noteworthy that the active device identification in this MC-CDMA-based approach might be easier than that in the precoded SIMA-based approach. That is, the AP only needs to identify $M = 6$ active devices among $L = K = 64$ devices in this MC-CDMA-based approach, while the AP in the precoded SIMA-based approach should identify $M = 6$ active devices among $N_I = \binom{2L}{Q} = \binom{128}{3} \approx 3.4 \times 10^5$ possible devices.

Fig. 6 shows the performance of MC-CDMA and precoded SIMA when the EM algorithm is used for the joint identification and detection in stage II with $L = 64$, $M = 6$, $P = 3$, and $Q = 3$. We can see that the probability of unsuccessful identification decreases with the SNR and the performance can be improved through iterations as shown in Fig. 6(a). For MC-CDMA, we assume perfect CSI. For the MC-CDMA-based approach, the OMP algorithm is used to identify $M = 6$ active devices without using the EM algorithm. Thus, for a fair comparison in terms of active device identification performance, the performance of precoded SIMA without iterations and with perfect CSI (the dashed line with square marks) can be compared with that of MC-CDMA (the solid line). We can see that precoded SIMA outperforms MC-CDMA as shown in Fig. 6(b), although it has to identify $M = 6$ active devices among approximately 3.4×10^5 possible devices, not $L = 64$ devices. Furthermore, it can also have a better performance through iterations using the EM algorithm. This performance behavior of the precoded SIMA is valid for both cases of perfect and imperfect CSI.

In Fig. 6(b), the performance of signal detection for the case of correct identification is shown with bit error rate (BER).

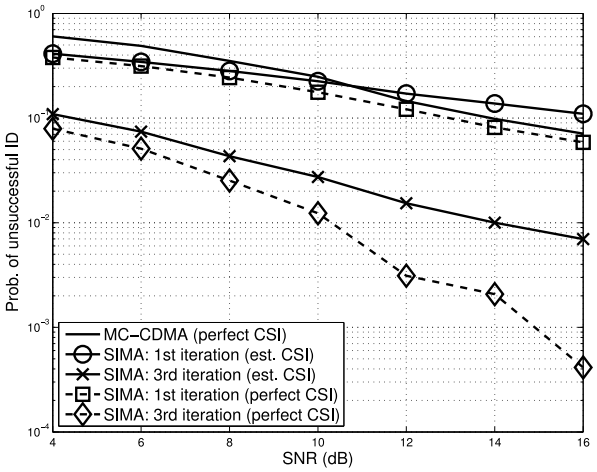

(a)

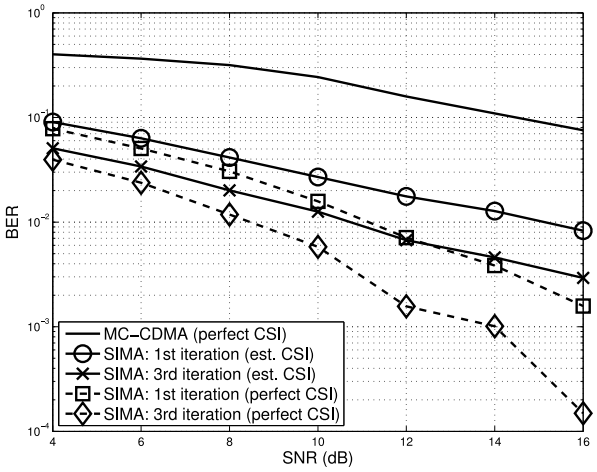

(b)

Fig. 6. Performances of the joint identification and detection in stage II for various SNRs when $L = 64$, $M = 6$, $P = 3$, and $Q = 3$. (a) Probability of unsuccessful identification. (b) BER.

At a low SNR, the BER performances of perfect CSI and imperfect CSI are not significantly different. However, as the SNR increases, the performance gap grows. It is noteworthy that the NMSE is fixed as 0.05 for imperfect CSI regardless of the SNR in this simulation. Since the NMSE decreases with the SNR as shown in Fig. 3, we could expect a better performance than that in Fig. 6(b) when the NMSE decreases with the SNR. We can also see that the BER performance is improved through iterations and the BER performance of MC-CDMA (with perfect CSI) is worse than that of precoded SIMA.

In order to see the impact of iterations in the EM algorithm, we show the probability of unsuccessful identification for various number of iterations in Fig. 7 when $L = 64$, $M = 6$, $P = 3$, $Q = 3$, and SNR $\in \{6, 10, 14\}$ dB. We can see that three iterations might be sufficient for reasonably high SNRs.

Fig. 8 shows the simulation results for various numbers of subcarriers, L, when $M = 3$, $P = 3$, $Q = 3$, and SNR $= 12$ dB. The probability of unsuccessful identification decreases with L when $L \leq 64$ and it can be sufficiently low (less than 10^{-2}) through iterations although the CSI is imperfect as shown in Fig. 8(a). It is also shown that the BER performance can be improved through iterations and by increasing L as shown in Fig. 8(b).

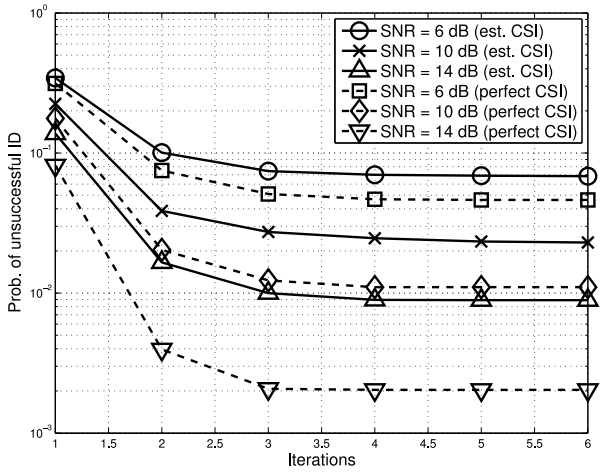

Fig. 7. Performance improvement of the EM algorithm over iterations in terms of the probability of unsuccessful identification when when $L = 64$, $M = 6$, $P = 3$, and $Q = 3$.

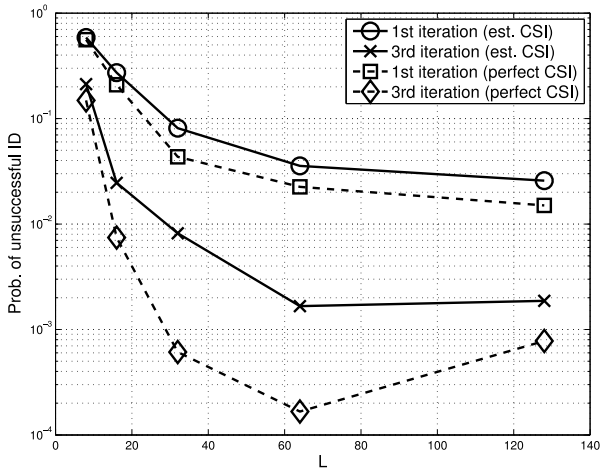

(a)

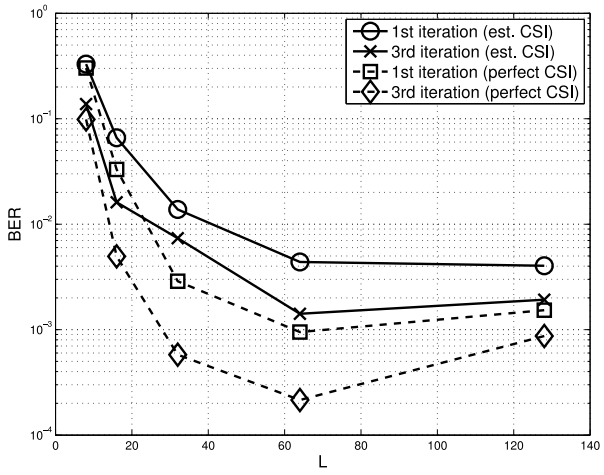

(b)

Fig. 8. Performances of the joint identification and detection in stage II for various values of L when $M = 3$, $P = 3$, $Q = 3$, and SNR $= 12$ dB. (a) Probability of unsuccessful identification. (b) BER.

VI. Conclusion

We introduced SIMA and applied it to uplink access in a wireless system of a large number of devices with low activity to exploit the sparsity of active devices as well as identification vectors for efficient identification of them. A two-stage scheme was proposed to receive signals from active devices with their identifications. In stage I, active devices transmit randomly chosen uplink pilot signals to allow the AP to estimate their CSI. In stage II, the AP perform coherent detection to not only detect data symbols, but also identify active devices with their unique identification sequences, SIVs. We derived computationally efficient methods for the channel estimation of active devices in stage I and for the joint identification and detection in stage II by modifying the OMP algorithm. Simulation results have shown that the proposed two-stage transmission scheme can be effectively employed to the system of many devices for wireless IoT and it can estimate the CSI of active devices under reasonable conditions and identify them with SIVs well.

References

[1] *Y.2060: Overview of the Internet of Things*, ITU-T, Geneva, Switzerland, Jun. 2012.

[2] C. Tang *et al.*, "Comparative investigation on CSMA/CA-based opportunistic random access for Internet of Things," *IEEE Internet Things J.*, vol. 1, no. 2, pp. 171–179, Apr. 2014.

[3] M. Mohan and S. Sudharman, "GALS with CDMA based access scheduling for wireless Internet of Things," in *Proc. Int. Conf. Control Instrum. Commun. Comput. Technol. (ICCICCT)*, Jul. 2014, pp. 409–413.

[4] Y. Chen *et al.*, "Time-reversal wireless paradigm for green Internet of Things: An overview," *IEEE Internet Things J.*, vol. 1, no. 1, pp. 81–98, Feb. 2014.

[5] M. Hasan, E. Hossain, and D. Niyato, "Random access for machine-to-machine communication in LTE-advanced networks: Issues and approaches," *IEEE Commun. Mag.*, vol. 51, no. 6, pp. 86–93, Jun. 2013.

[6] *Study on RAN Improvments for Machine-Type Communications*, 3GPP TR 37.868 V11.0, Oct. 2011.

[7] M. Condoluci, M. Dohler, G. Araniti, A. Molinaro, and K. Zheng, "Toward 5G densenets: Architectural advances for effective machine-type communications over femtocells," *IEEE Commun. Mag.*, vol. 53, no. 1, pp. 134–141, Jan. 2015.

[8] A. K. Fletcher, S. Rangan, and V. K. Goyal, "On-off random access channels: A compressed sensing framework," *CoRR*, vol. abs/0903.1022, 2009.

[9] H. Zhu and G. B. Giannakis, "Exploiting sparse user activity in multiuser detection," *IEEE Trans. Commun.*, vol. 59, no. 2, pp. 454–465, Feb. 2011.

[10] L. Applebaum, W. U. Bajwa, M. F. Duarte, and R. Calderbank, "Asynchronous code-division random access using convex optimization," *Phys. Commun.*, vol. 5, no. 2, pp. 129–147, 2012.

[11] F. Fazel, M. Fazel, and M. Stojanovic, "Random access compressed sensing over fading and noisy communication channels," *IEEE Trans. Wireless Commun.*, vol. 12, no. 5, pp. 2114–2125, May 2013.

[12] J.-P. Hong, W. Choi, and B. D. Rao, "Sparsity controlled random multiple access with compressed sensing," *IEEE Trans. Wireless Commun.*, vol. 14, no. 2, pp. 998–1010, Feb. 2015.

[13] E. J. Candes and T. Tao, "Decoding by linear programming," *IEEE Trans. Inf. Theory*, vol. 51, no. 12, pp. 4203–4215, Dec. 2005.

[14] D. Donoho, "Compressed sensing," *IEEE Trans. Inf. Theory*, vol. 52, no. 4, pp. 1289–1306, Apr. 2006.

[15] R. Baraniuk, M. Davenport, R. DeVore, and M. Wakin, "A simple proof of the restricted isometry property for random matrices," *Constr. Approx.*, vol. 28, no. 3, pp. 253–263, 2008.

[16] Y. C. Eldar and G. Kutyniok, *Compressed Sensing: Theory and Applications*. Cambridge, U.K.: Cambridge Univ. Press, 2012.

[17] H. F. Schepker, C. Bockelmann, and A. Dekorsy, "Exploiting sparsity in channel and data estimation for sporadic multi-user communication," in *Proc. ISWCS*, Ilmenau, Germany, Aug. 2013, pp. 1–5.

[18] G. Wunder, P. Jung, and C. Wang, "Compressive random access for post-LTE systems," in *Proc. IEEE ICC*, Sydney, NSW, Australia, Jun. 2014, pp. 539–544.

[19] G. Wunder, H. Boche, T. Strohmer, and P. Jung, "Sparse signal processing concepts for efficient 5G system design," *IEEE Access*, vol. 3, pp. 195–208, 2015.

[20] J. Choi, "Sparse index multiple access," in *Proc. IEEE Glob. Conf. Signal Inf. Process. (GlobalSIP)*, Orlando, FL, USA, Dec. 2015, pp. 324–327.

[21] *IEEE Standards Association*, IEEE Standard 802.15.4-2006, 2012.

[22] W.-C. Wu and K.-C. Chen, "Identification of active users in synchronous CDMA multiuser detection," *IEEE J. Sel. Areas Commun.*, vol. 16, no. 9, pp. 1723–1735, Dec. 1998.

[23] D. Guo and C.-C. Wang, "Multiuser detection of sparsely spread CDMA," *IEEE J. Sel. Areas Commun.*, vol. 26, no. 3, pp. 421–431, Apr. 2008.

[24] R. Abu-Alhiga and H. Haas, "Subcarrier-index modulation OFDM," in *Proc. IEEE 20th Int. Symp. Pers. Indoor Mobile Radio Commun.*, Tokyo, Japan, Sep. 2009, pp. 177–181.

[25] E. Başar, U. Aygölü, E. Panayirci, and H. V. Poor, "Orthogonal frequency division multiplexing with index modulation," *IEEE Trans. Signal Process.*, vol. 61, no. 22, pp. 5536–5549, Nov. 2013.

[26] T. M. Cover and J. A. Thomas, *Elements of Information Theory*, 2nd ed. Hoboken, NJ, USA: Wiley, 2006.

[27] J. Choi and Y. Ko, "Compressive sensing based detector for sparse signal modulation in precoded OFDM," in *Proc. IEEE ICC*, London, U.K., Jun. 2015, pp. 4536–4540.

[28] C. Tepedelenlioglu, "Maximum multipath diversity with linear equalization in precoded OFDM systems," *IEEE Trans. Inf. Theory*, vol. 50, no. 1, pp. 232–235, Jan. 2004.

[29] J. Choi, "Low density spreading for multicarrier systems," in *Proc. IEEE 8th Int. Symp. Spread Spectr. Tech. Appl.*, Sydney, NSW, Australia, Aug. 2004, pp. 575–578.

[30] G. M. Davis, S. G. Mallat, and Z. Zhang, "Adaptive time-frequency decompositions," *Opt. Eng.*, vol. 33, no. 7, pp. 2183–2191, 1994.

[31] J. A. Tropp, "Greed is good: Algorithmic results for sparse approximation," *IEEE Trans. Inf. Theory*, vol. 50, no. 10, pp. 2231–2242, Oct. 2004.

[32] A. P. Dempster, N. M. Laird, and D. B. Rubin, "Maximum likelihood from incomplete data via the EM algorithm," *J. Roy. Stat. Soc. B*, vol. 39, no. 1, pp. 1–38, 1977.

[33] G. J. McLachlan and T. Krishnan, *The EM Algorithm and Extensions*. New York, NY, USA: Wiley, 1997.

Jinho Choi (SM'02) was born in Seoul, South Korea. He received the B.E. (*magna cum laude*) degree in electronics engineering from Sogang University, Seoul, in 1989, and the M.S.E. and Ph.D. degrees in electrical engineering from the Korea Advanced Institute of Science and Technology, Daejeon, South Korea, in 1991 and 1994, respectively.

He was a Professor/Chair of wireless with the College of Engineering, Swansea University, Swansea, U.K. He joined the Gwangju Institute of Science and Technology, Gwangju, South Korea, in 2013, where he is a Professor. He authored two books published by Cambridge University Press in 2006 and 2010. His current research interests include wireless communications and array/statistical signal processing.

Prof. Choi was a recipient of the 1999 Best Paper Award for Signal Processing from EURASIP, and the 2009 Best Paper Award of the WPMC Conference. He is currently an Editor of the IEEE TRANSACTIONS ON COMMUNICATIONS and had served as an Associate Editor or an Editor of other journals, including for IEEE COMMUNICATIONS LETTERS, the *Journal of Communications and Networks*, the IEEE TRANSACTIONS ON VEHICULAR TECHNOLOGY, and the *ETRI Journal*.